Chapter 3:

Evaluation of a Technetium-99m Labeled Bombesin Homodimer for GRPR Imaging in Prostate Cancer

Zilin Yu
Giuseppe Carlucci
Hildo J.K. Ananias
Rudi A. J.O. Dierckx
Shuang Liu
Wijnand Helfrich
Fan Wang
Igle Jan de Jong
Philip H. Elsinga

Amino Acids. 2013 Feb; 44(2):543-53

ABSTRACT

Introduction: Multimerization of peptides can improve the binding characteristics of the tracer by increasing local ligand concentration and decreasing dissociation kinetics. In this study, a new bombesin homodimer was developed based on a ε-aminocaproic acid-bombesin(7-14) (Aca-bombesin(7-14)) fragment which has been studied for targeting the gastrin-releasing-peptide-receptor (GRPR) in prostate cancer. Methods: The bombesin homodimer was conjugated to 6-Hydrazinopyridine-3-carboxylic acid (HYNIC) and labeled with ^{99m}Tc for SPECT imaging. The *in vitro* binding affinity to GRPR, cell uptake, internalization and efflux kinetics of the radiolabelled bombesin dimer were investigated in the GRPR-expressing human prostate cancer cell line PC-3. Biodistribution and the GRPR targeting potential were evaluated in PC-3 tumor-bearing athymic nude mice. Results: When compared to the bombesin monomer, the binding affinity of the bombesin dimer is about 10 times lower. However the ^{99m}Tc labeled bombesin dimer showed a three times higher cellular uptake at 4 hours after incubation, but similar internalization and efflux characters *in vitro*. Tumor uptake and *in vivo* pharmacokinetics in PC-3 tumor bearing mice were comparable. The tumor was visible on the dynamic images in the first hour and could be clearly distinguished from non-targeted tissues on the static images after 4 hours. Conclusion: The GRPR targeting ability of the ^{99m}Tc labeled bombesin dimer was proven *in vitro* and *in vivo*. This bombesin homodimer provides a good starting point for further studies on enhancing the tumor targeting activity of bombesin multimers.

INTRODUCTION

Prostate cancer is one of the most common cancers in men in the USA and in Europe(1-2). In the course of the disease bone metastases will develop in the majority of cases with advanced prostate cancer. This number will reach 90% in patients with castrate resistant prostate cancer treated with chemotherapy (3). At present there is an unmet need to measure response to treatment of prostate cancer metastases in the skeleton. With a specific radiotracer and specific target in the tumor, positron emission tomography (PET)

and single photon emission computed tomography (SPECT) would be powerful diagnostic tools in detection of prostate cancer. The Gastrin-Releasing-Peptide Receptor (GRPR) is a subtype of the bombesin receptor family. Mammalian GRPR is preferentially expressed in non-neuroendocrine tissues of the breast and pancreas and in neuroendocrine cells of the brain, gastrointestinal tract, and lung (4-8). It has also been shown that GRPR is overexpressed in a large variety of human tumors, including prostate, breast, renal and (non) small cell lung cancer. Due to the enhanced expression of GRPR in prostate cancer, GRPR is considered as a potential target for the diagnosis, staging or treatment of prostate cancer. Bombesin is a 14 amino acid peptide which was first isolated from the skin of frogs in the 1970 (9). Bombesin and its mammalian counterpart share 7 identical amino acid residues at the C-terminal, which was identified as the binding domain of the bombesin receptor (10).

Radiolabeled bombesin analogs have proven their GRPR binding ability in several cancer cell lines and in various tumor models (11–14). Previously, an ε-aminocaproic acid (Aca) modified bombesin analogue was labeled with ^{18}F and the compound was evaluated in a prostate cancer animal model (11). Although ^{18}F-FB-Aca-Bombesin(7–14) showed its ability to target GRPR in an animal model, due to the lipophilic character of the tracer detection of the orthotopic prostate cancer was hampered by high abdominal background levels. Recently, we developed HYNIC conjugated Aca-BN(7–14) and labeled it with ^{99m}Tc for SPECT imaging of prostate cancer in an animal model (15). Compared to ^{18}F-FB-Aca-Bombesin(7–14), ^{99m}Tc-HYNIC(Tricine/TPPTS)-Aca-BN(7–14) (^{99m}Tc-HABN) showed reduced abdominal background and improved tumor-to-normal-tissue (T/NT) contrast (tumor-to-muscle ratio from lower than 5 increased to 13.9 ± 5.9 at 1 hour post injection) on SPECT images. While most bombesin-like peptides are monomers, we applied the dimerization technology and synthesized a new dimeric bombesin with 2 identical Aca-Bombesin(7–14) units. Multivalent interactions are frequently found in nature where they increase the affinity of weak ligand–receptor interactions such as in the DNA-DNA duplex formation by multiple weak interactions between individual complementary nucleotides, or the typical Y-shaped antibody composed of two heavy chains and two light chains which are joined by disulfide linkages (16–19). Multivalent structures have become a

strategy for the development of drugs and diagnostic agents. It has been shown by several research groups that multivalent compounds are able to enhance the interaction between the ligand and corresponding receptor (20–25). One of the most prominent examples are multivalent Arginine-Glycine-Aspartic acid (RGD) analogues. Several isotopes (^{99m}Tc, ^{111}In, ^{18}F, ^{68}Ga, etc) and chelators (HYNIC, DOTA, DTPA, etc) have been applied for the preparation of dimeric and tetrameric RGD tracers (21–24,26). The binding affinity is significantly increased at higher orders of binding valency, a principle usually referred to as avidity. The aim of this study is to investigate the GRPR targeting characteristics of the bombesin homodimer as a potential imaging agent for prostate cancer.

MATERIALS AND METHODS

Chemicals

Tricine (N-(Tri(hydroxymethyl)methyl)glycine) was purchased from Sigma/Aldrich (St. Louis, Missouri, USA). Trisodium triphenylphosphine-3,3',3''-trisulfonate (TPPTS) was purchased from Alfa Aesar (Karlsruhe, Germany). Both were used without further purification. The peptide Glu[Aca-BN(7-14)]$_2$ was provided by Peptides International (Louisville, KY, USA). Na^{99m}TcO$_4$ was eluted from the ^{99}Mo/^{99m}Tc generator MTcG-4 (IAE Radioisotope Centre POLATOM, Świerk, Poland). ^{125}I-Tyr^4-BN was obtained from Perkin-Elmer Life and Analytical Sciences (Waltham, Massachusetts, USA).

Equipment

Semi-preparative reversed-phase high-performance liquid chromatography (RP-HPLC) was performed on a HITACHI L-2130 HPLC system (Hitachi High Technologies America Inc., Pleasanton, California, USA) equipped with a Bicron Frisk-Tech area monitor. Isolation and quality control of ^{99m}Tc-HYNIC(Tricine/TPPTS)-Glu[Aca-BN(7-14)]$_2$ (^{99m}Tc-HABN$_2$) were performed using a Phenomenex reversed-phase Luna C18 column (10 mm × 250 mm, 5 µm) (Torrance, California, USA). The flow was set at 2.5 mL/min using a gradient system starting from 90% solvent A (0.01 M phosphate buffer, pH=6.0) and 10% solvent B

(acetonitrile) (5 minutes) and ramped to 45% solvent A and 55% solvent B at 35 minutes (HPLC Method 1).

HPLC Method 2 used a LabAlliance semi-preparative HPLC system equipped with a UV-Vis detector (λ = 254 nm) and Zorbax C18 semi-prep column (9.4 mm x 250 mm, 100 Å pore size). The flow rate was 2.5 mL/min. The mobile phase was isocratic with 60% solvent A (0.1% acetic acid in water) and 40% solvent B (0.1% acetic acid in acetonitrile) at 0 – 5 min, followed by a gradient mobile phase going from 60% solvent A and 40% solvent B at 5 min to 20% solvent A and 80% solvent B at 30 min. HPLC Method 3 used a LabAlliance semi-preparative HPLC system equipped with a UV-Vis detector (λ = 254 nm) and Zorbax C18 semi-preparative column (9.4 mm x 250 mm, 100 Å pore size). The flow rate was 2.5 mL/min. The gradient mobile phase goes from 90% solvent A (0.1% acetic acid in water) and 10% solvent B (0.1% acetic acid in acetonitrile) at 0 min to 75% solvent A at 5 min, followed by a gradient mobile phase going from 75% solvent A to 65% solvent A at 40 min.

Synthesis of HYNIC-Glu[Aca-BN(7-14)]$_2$

Sodium succinimidyl 6-(2-(2-sulfonatobenzaldehyde)hydrazono)nicotinate (HYNIC-NHS) was prepared according to literature method (Harris et al. 1999). HYNIC-NHS (21.8 mg, 50 µmol) and Glu[Aca-BN(7-14)]$_2$ (5.8 mg, 2.6 µmol) were dissolved in 1.5 mL of DMF. The pH was adjusted to 8.5 – 9.0 with DIPEA. The mixture was stirred for 7 days at room temperature to make sure that the reaction was complete as indicated by the disappearance of the peptide peak. The product was purified by HPLC (Method 1). The peak of interest at ~28 min was collected. The collected fractions were combined, and lyophilized to obtain 1.7 mg product, which was re-purified by HPLC (Method 2). Fraction at ~32.5 min was collected. Lyophilization of the collected fractions gave the final product 0.8 mg (13%) with the purity > 95% by HPLC. ESI-MS: $C_{114}H_{161}N_{33}O_{27}S_3$, calculated 2521.9, observed 2522 ($[M+H]^+$).

Radiochemistry

100 µL of the HYNIC-Glu[Aca-BN(7-14)]$_2$ solution (1 mg/mL in H_2O), 100 µL of tricine solution (50 mg/mL in 25 mM succinate buffer, pH 5.0), 100 µL of TPPTS solution (50 mg/mL in 25 mM succinate buffer, pH 5.0), 5 µL of $SnCl_2$ solution (3.0 mg/mL in 0.1 N HCl) and 100 µL of $Na^{99m}TcO_4$ (370 MBq) in saline were added to a 1.5 mL Eppendorf cup. The Eppendorf cup containing the reaction mixture was sealed and heated at 95 °C for 20 min. After cooling to room temperature, the mixture was purified by HPLC (Method 1). The product was then passed through a Waters Sep-Pak C18 light cartridge. ^{99m}Tc-HABN$_2$ was eluted with ethanol (0.4 mL) and diluted with saline solution for *in vitro* and *in vivo* experiments. A sample of the resulting solution was analyzed by the same HPLC system (method 1).

Partition Coefficient

The partition coefficient was determined using the method described previously (15). The tracer was dissolved in a mixture of 0.5 mL *n*-octanol and 0.5 mL 25 mM phosphate buffer (pH 7.4) and well mixed for 5 min at room temperature. Then the mixture was centrifuged at 3000 rpm for 5 minutes. 100 µL samples were obtained from *n*-octanol and aqueous layers. All samples were counted in a *γ*-counter (Compugamma CS1282, LKB-Wallac, Turku, Finland). The *log D* value is reported as an average of three different measurements.

In Vitro Stability

The tracer was dissolved in 1 mL saline or L-Cysteine solution (1 mg/mL), incubated at room temperature and analyzed by HPLC (Method 1) at 1, 2, 4, 6, and 24 hours post incubation. Human serum from healthy donors was incubated at 37 °C with ^{99m}Tc-HABN$_2$ for different time periods (1, 2, 4, 6, 24 h). After incubation, a sample of 250 µL was precipitated with 750 µL acetonitrile/ethanol ($V_{acetonitrile}/V_{ethanol}$ =1:1) and then centrifuged (3 minutes at 3000 rpm), the supernatants were passed through a Millex-LG filter (Millipore, Co. Cork, Carrigtwohill, Ireland) and afterwards analyzed by HPLC (Method 1). Results were plotted as radiochemical purity (RCP) at different time-points.

Cell Culture

The GRPR-positive human prostate cancer cell line PC-3 (ATCC, Manassas, Virginia, USA) was cultured in RPMI 1640 (Lonza, Verviers, France) supplemented with 10% fetal calf serum (Thermo Fisher Scientific Inc., Logan, Utah, USA) at 37 °C in a humidified 5% CO_2 atmosphere.

In Vitro Competitive Receptor Binding Assay

The *in vitro* GRPR binding affinities of Glu[Aca-BN(7-14)]$_2$ and HYNIC-Glu[Aca-BN(7-14)]$_2$ were assessed via a competitive displacement assay with ^{125}I-Tyr^4-BN(1-14) as the GRPR specific radioligand. Experiments were performed with PC-3 human prostate cancer cells according to a method previously described (15). The 50% inhibitory concentration (IC_{50}) values were calculated by fitting the data with nonlinear regression using GraphPad Prism 5.0 (GraphPad Software, San Diego, California, USA). Experiments were performed with triplicate samples. IC_{50} values are reported as an average of these samples plus the standard deviation (SD).

Cellular uptake studies

One day prior to the assay, PC-3 cells at confluence were placed in 6-well plates (0.5 million cells/well). The cells were washed twice with PBS solution before using for the experiments. ^{99m}Tc-HABN or ^{99m}Tc-HABN$_2$ (0.0037 MBq/well) was incubated with cells at 37 °C for 0, 15, 30, 45, 60, 90, 120 or 240 minutes in triplicate to allow for cellular uptake. 20 µg of unlabelled Glu[Aca-BN(7-14)]$_2$ was co-incubated with ^{99m}Tc-HABN or ^{99m}Tc-HABN$_2$ in blocking groups. To remove unbound radioactivity, the cells were washed twice with ice-cold PBS and the cells were lysed by incubation with 1 M NaOH at 37 °C. The resulting lysate in each well was aspirated to determine the uptake of activity with a γ-counter. Results are expressed as percentage of incubated radioactivity (mean±SD).

Internalization and efflux Studies

For the internalization study, 1 million PC-3 cells were placed in 6-well plates before the experiments and kept at 37 °C overnight. The cells were washed with PBS and then incubated with ^{99m}Tc-HABN$_2$ (0.0037 MBq/well) for 2 hours at 4 °C. To remove unbound radioactivity, the cells were washed twice with ice-cold PBS and incubated with the pre-warmed culture medium at 37 °C for 0, 5, 15, 30, 45, 60, 90 and 120 minutes in triplicate to allow for internalization. To remove cell-surface bound radiotracer, the cells were washed twice for 3 minutes with acid (50 mM glycine−HCl/100 mM NaCl, pH 2.8). The acid solution was collected and measured with a γ-counter. The results were collected as the surface-bound activity. Subsequently, the cells were lysed by incubation with 1 M NaOH at 37 °C and the resulting lysate in each well was measured to determine the internalized radioactivity with γ-counter. Results are expressed as the percentage of total radioactivity (internalized activity / (surface-bound activity + internalized activity)), (mean±SD). For the efflux study, 1 million PC-3 cells were placed in 6-well plates 1 day before the experiments and kept at 37 °C. The cells were washed with PBS and then incubated with ^{99m}Tc-HABN$_2$ (3.7 KBq/well) for 1 hour at 37 °C to allow for maximum internalization. To remove unbound radioactivity, the cells were washed twice afterwards with ice-cold PBS and were then incubated in the pre-warmed culture medium at 37 °C for 0, 15, 30, 45, 60, 90, 120, and 240 minutes in triplicate to allow for externalization. To remove cell-surface bound radiotracer, the cells were washed twice for 3 minutes with acid (50 mM glycine−HCl/100 mM NaCl, pH 2.8). Then, the cells were lysed by incubation with 1 N NaOH at 37 °C, and the resulting lysate in each well was aspirated to determine the remaining radioactivity in a γ-counter. Results are expressed as the percentage of maximum intracellular radioactivity (remaining activity at specific time-point / activity at time-point 0) (mean±SD).

Animal Model

In the PC-3 tumor model, 2 × 10^6 PC-3 cells (suspended in 0.1 mL sterile saline) were subcutaneous injected into the left front flank of male athymic mice (Harlan, Zeist, The

Netherlands). During the injection, animals were anesthetized with a gas composed of ~3.5% isoflurane in an air/oxygen mixture. The mice were used for biodistribution experiments and microSPECT and CT imaging when the tumor volume reached a mean diameter of 0.8-1.0 cm (typically 3-4 weeks after tumor inoculation). All animal experiments were performed in accordance with the regulations of Dutch law on animal welfare and the institutional ethics committee for animal procedures approved the protocol.

MicroSPECT imaging and Biodistribution

The subcutaneous tumor bearing mice were separated into 4 groups (4 animals per group) and used for imaging and biodistribution when the tumor volume reached 250-300 mm^3 (4-5 weeks after inoculation). MicroSPECT scans were performed on a three-head γ-camera (MILabs, U-SPECT-II, Utrecht, The Netherlands) equipped with a multi-pinhole high-resolution collimator. For the microSPECT scans ~30MBq ^{99m}Tc-$HABN_2$ were administered by penis vein injection under isoflurane anesthesia. 60 min of dynamic microSPECT data was acquired immediately after injection. Mice (group 1) that were used for dynamic scanning were sacrificed directly after the scan with an overdose of isoflurane anesthesia. CT scan and biodistribution were performed afterwards. Blood, tumor, major organs and tissue samples were collected, weighted and counted by γ-counter. The percentage of injected dose per gram (%ID/g) was determined for each sample. For each mouse, radioactivity of the tissue samples was calibrated against a known aliquot of radiotracer. For static imaging, mice were sacrificed at 4 (group 2) and 24 h (group 3) after injection. Afterwards, 60-min microSPECT and microCT images were acquired. Biodistribution was performed as described above.

For the receptor-blocking experiment 300 μg of unlabeled Aca-BN(7-14) was pre-injected 30 min before the tracer injection. The animals of the blocking group (group 4) were sacrificed and 60-min static microSPECT & CT images were acquired at 4 hours after tracer injection. Biodistribution was performed after the CT scan. Images were reconstructed by using U-SPECT-Rec v 1.34i3 (MILabs, Utrecht, the Netherlands) with a pixel-based

ordered-subsets expectation maximum (POSEM) algorithm. Final images were 1 mm slices, made with Amide 0.9.1 (open source software).

Statistical Analysis

Quantitative data are expressed as mean ± SD. Means were compared using the Student t test. *P* values <0.05 were considered as significant.

RESULTS

Synthesis, Radiolabeling, Partition Coefficient and *In Vitro* Stability

^{99m}Tc-HABN$_2$ (figure 1) was prepared at 95 °C with moderate labeling yield (>80%). After purification the radiochemical purity was higher than 95%. The specific activity was ~17.4 ± 9.7 GBq/µmol (n=7). ^{99m}Tc-HABN$_2$ was well separated from precursor using HPLC system. The retention time (HPLC Method 1) of ^{99m}Tc-HABN$_2$ and HYNIC-Glu[Aca-BN(7-14)]$_2$ was around 28 and 24 min, respectively. The partition coefficient was determined in a mixture of *n*-octanol and phosphate buffer (pH=7.4). The *log D* value of ^{99m}Tc-HABN$_2$ was -1.54 ± 0.16. The *in vitro* stability of ^{99m}Tc-HABN$_2$ was evaluated in saline, human serum and in the presence of excess L-Cysteine (1.0 mg/mL, pH 7.4) (figure 2). ^{99m}Tc-HABN$_2$ was stable in the presence of excess L-Cysteine and human serum for at least 4 hours (RCP> 95 %). The RCP of ^{99m}Tc-HABN$_2$ in serum slowly decreased to ~84% after 24 hours.

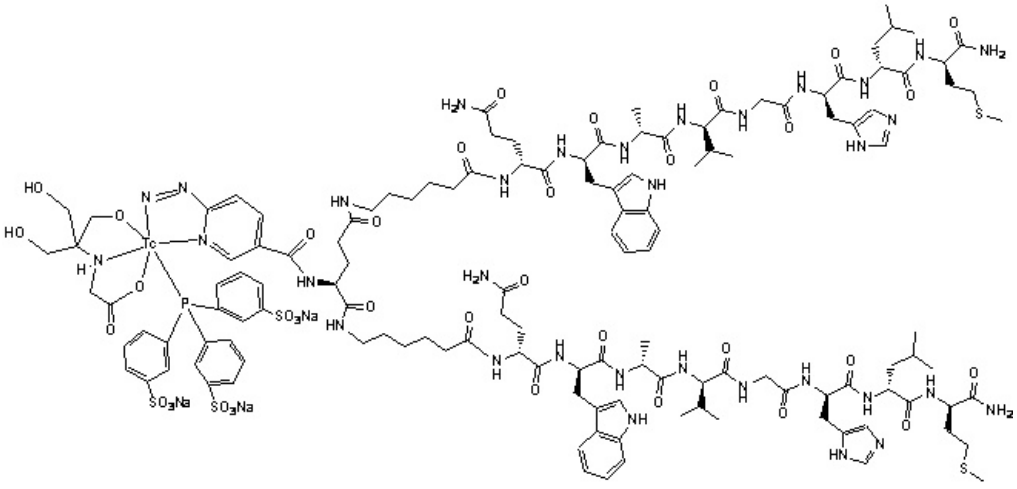

Figure 1: ^{99m}Tc-HYNIC(Tricine/TPPTS)-Glu[Aca-BN(7-14)]$_2$

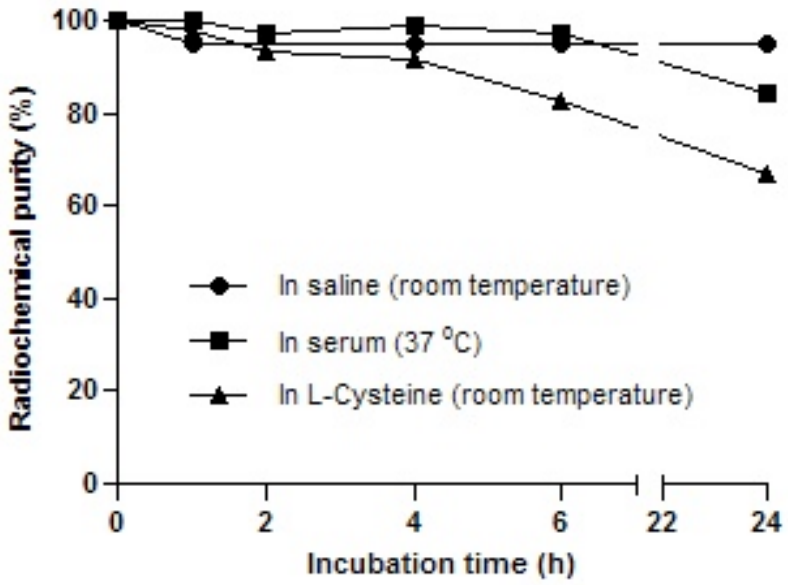

Figure 2: *In vitro* stability of ^{99m}Tc-HABN$_2$ in saline (at room temperature), human serum (at 37 ^{o}C) and L-Cysteine (at room temperature). Results are plotted as the radiochemical purity at different time points

In vitro Competitive Receptor Binding Assay

Using ^{125}I-Tyr^4-BN(1-14) as GRPR specific radioligand, the binding affinities of Glu[Aca-BN(7-14)]$_2$ and HYNIC-Glu[Aca-BN(7-14)]$_2$ for GRPR were compared via an in vitro competitive binding assay. Results are plotted as sigmoid curves for the displacement of ^{125}I-Tyr^4-BN(1-14) as a function of increasing concentrations of Glu[Aca-BN(7-14)]$_2$, and HYNIC-Glu[Aca-BN(7-14)]$_2$ (figure 3). The IC_{50} values were found to be 31.4 ± 0.4 nM and 63.4 ± 11.7 nM for Glu[Aca-BN(7-14)]$_2$ and HYNIC-Glu[Aca-BN(7-14)]$_2$, respectively.

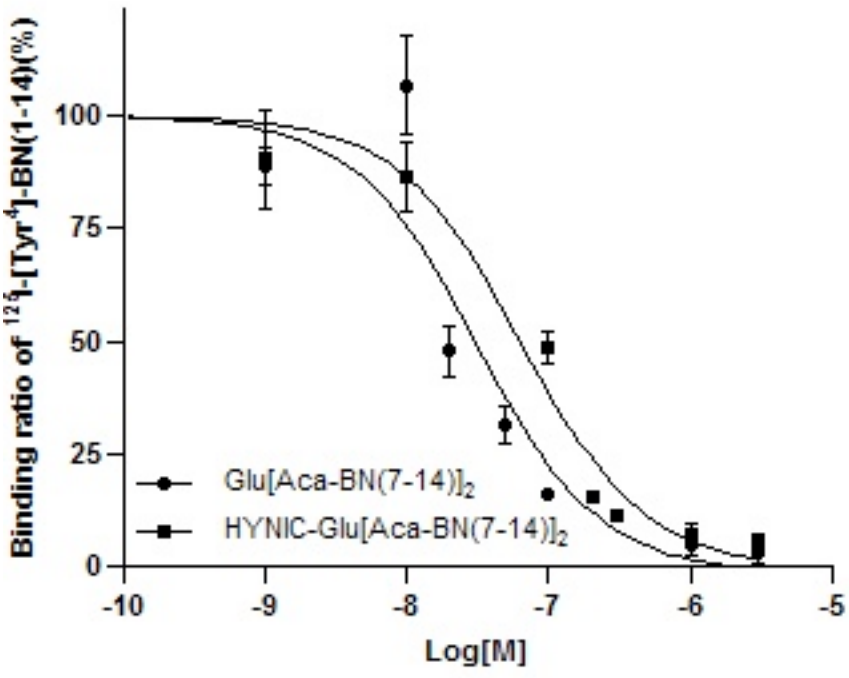

Figure 3: Inhibition of ^{125}I-[Tyr^4]-BN(1-14) binding to GRPR on PC-3 cells by Glu[Aca-BN(7-14)]$_2$ and HYNIC-Glu[Aca-BN(7-14)]$_2$. Log [M] = log of increasing concentration (mol/L) of Glu[Aca-BN(7-14)]$_2$ and HYNIC-Glu[Aca-BN(7-14)]$_2$

Cellular uptake studies

The *in vitro* uptake of ^{99m}Tc labeled bombesin monomer and dimer in PC-3 cells are shown in Figure 4. Compared to ^{99m}Tc-HABN, ^{99m}Tc-HABN$_2$ has slower cellular uptake within 30 min of incubation, but keeps accumulating in PC-3 cells over the 4 hours experiment period. The highest cellular uptake for ^{99m}Tc-HABN and ^{99m}Tc-HABN$_2$ is 10.9 ± 0.7 % (1 hour post incubation) and 32.5 ± 1.8 % (4 hours post incubation) of added radioactivity, respectively. Co-incubation with excess unlabeled bombesin significantly reduced the cellular uptake of both tracers (<1% of added activity was belonging to non-specific uptake).

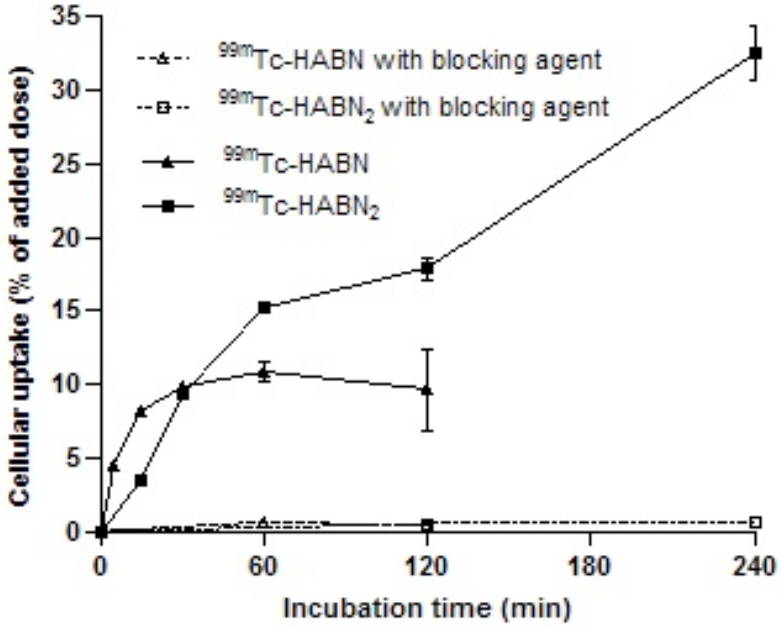

Figure 4: Cellular uptake assay of ^{99m}Tc-HABN and ^{99m}Tc-HABN$_2$ in PC-3 cells. The cellular uptake results were expressed as percentage added dose (n=3, mean ± SD)

Internalization and Efflux Studies

The internalization study depicted in figure 5A showed rapid internalization of ^{99m}Tc-HABN$_2$ into PC-3 cells within 5 minutes incubation. The portion of intracellular activity reached a plateau at 15 min post incubation and 80% of cell bound activity internalized into the cells. The results of the efflux study is shown in figure 5 B. For ^{99m}Tc-HABN$_2$, steady efflux was observed within 2 hours incubation. About 60% of the intracellular radioactivity was maintained in the cells at the end of the 4 hours experiment period. The efflux half-life of ^{99m}Tc-HABN$_2$ was 84 min.

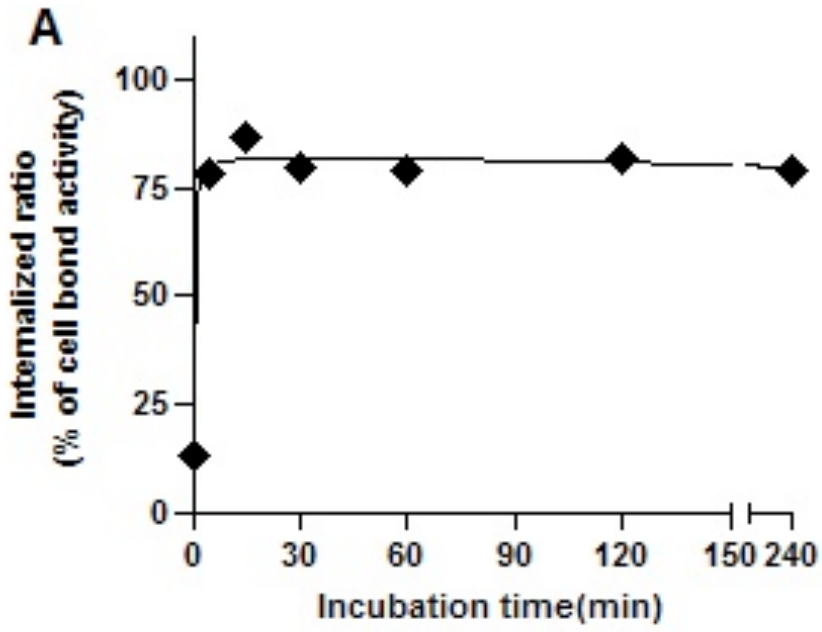
A
Internalized ratio
(% of cell bond activity)
100
75
50
25
0
0
30
60
90
120
150
240
Incubation time(min)

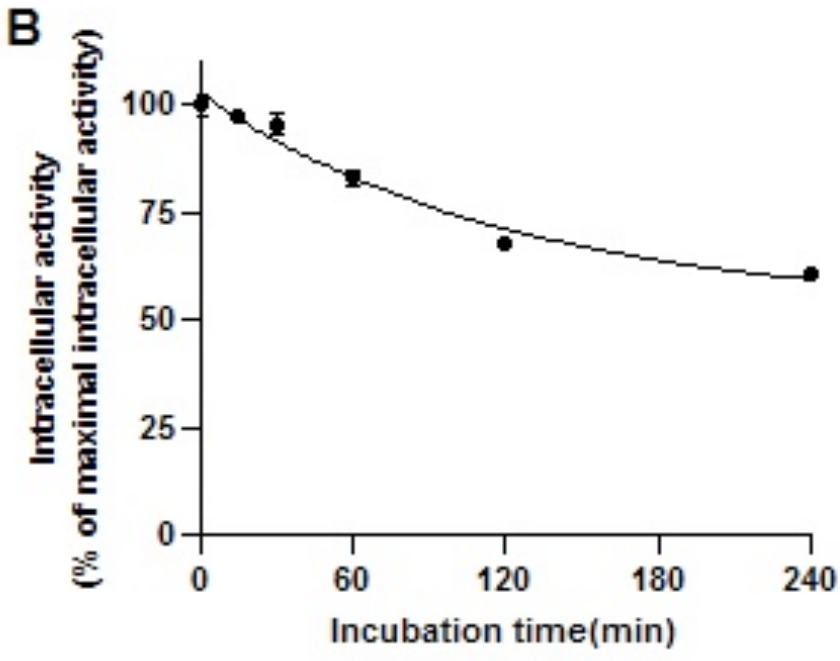
B
Intracellular activity
(% of maximal intracellular activity)
100
75
50
25
0
0
60
120
180
240
Incubation time(min)

Figure 5: Internalization (A) and efflux (B) kinetics of ^{99m}Tc-HABN$_2$ in PC-3 cell line (n=3, mean ± SD).

Biodistribution Experiments

Biodistribution of ^{99m}Tc-HABN$_2$ was evaluated in athymic nude mice bearing subcutaneous PC-3 tumors after performing the microSPECT and CT scans. The results are shown in Figure 6. Tumor uptake of ^{99m}Tc-HABN$_2$ was 1.58 ± 0.18 %ID/g at 60 min after injection, with a steady decrease to 0.47 ± 0.13 %ID/g at 24 h after injection. The highest radioactivity uptake (15.1±6.4 %ID/g) in kidney was observed at 4 h post injection. The tracer has low blood uptake and was cleared from blood rapidly. The uptake of ^{99m}Tc-HABN$_2$ in non-targeting organs (except kidney and pancreas) such as liver, bone, intestines was lower than 3 %ID/g and washed out rapidly. Due to the slower washout from tumor compared to normal-tissue, the T/NT ratio increased during the 24 h experiment period. The tumor-to-muscle ratio increased from 3.7 ± 1.1 at 1h after injection to 24.1 ± 21.5 at 24 h after injection. For determining the specificity of ^{99m}Tc-HABN$_2$ binding to GRPR, an excess of unlabeled Aca-BN(7-14) (300 µg/mouse) was injected before the tracer injection. At 4 hours post injection, the radioactivity accumulation was substantially reduced in tumor (from 0.8 ± 0.3 %ID/g to 0.4 ± 0.1 %ID/g) and pancreas (from 9.6 ± 7.6 %ID/g to 3.1 ± 0.2 %ID/g).

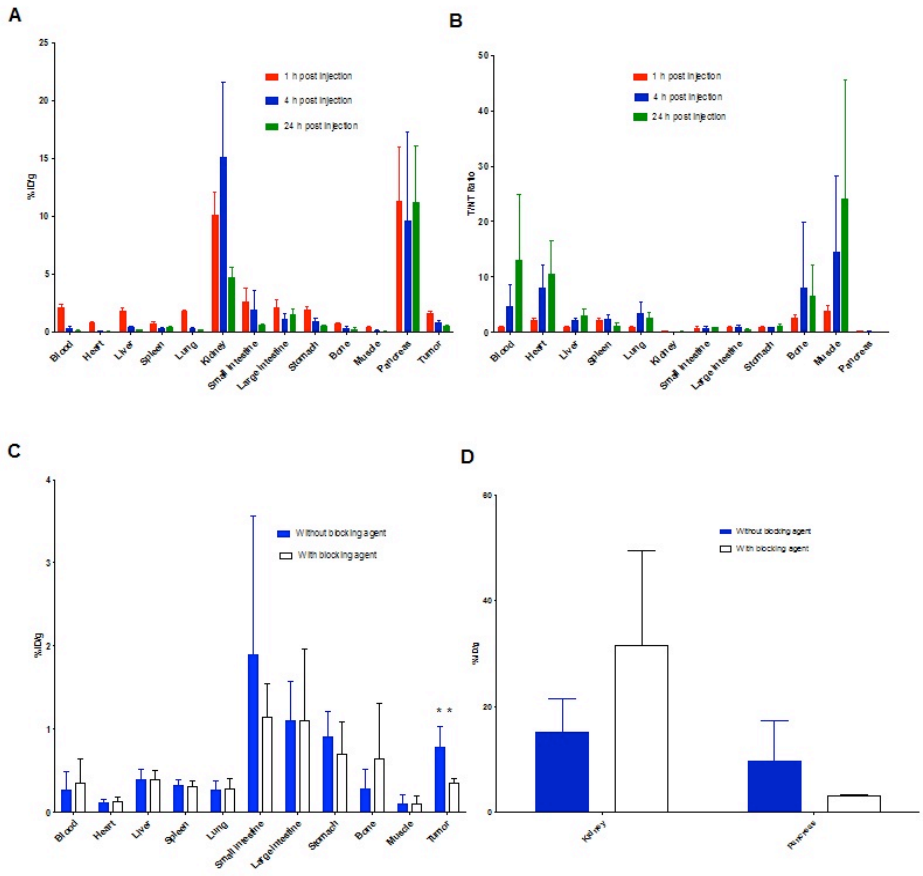

Figure 6: (A) Biodistribution of ^{99m}Tc-HABN$_2$ at 1, 4, 24 hours postinjection in athymic nude mice bearing subcutaneous PC-3 tumor (mean ± SD %ID/g), (B)T/NT ratio of ^{99m}Tc-HABN$_2$ at 1, 4, 24 hours postinjection (mean ± SD), (C) Biodistribution of ^{99m}Tc-HABN$_2$ at 4 hours postinjection with and without blocking agent (mean ± SD %ID/g), (D) Uptake of ^{99m}Tc-HABN$_2$ in kidney and pancreas at 4 hours postinjection with and without blocking agent (mean ± %ID/g); *= statistically significant difference (p<0.05).

MicroSPECT Imaging

Typical microSPECT images of PC-3 tumor bearing mice at different time points after tracer injection are shown in figure 7. The tumors were clearly visible from static miroSPECT images acquired at 4 hours after injection of ^{99m}Tc-HABN$_2$ (B). Prominent uptake of ^{99m}Tc-HABN$_2$ was also observed in the kidneys and pancreas at all images during

the 4 h experiment period (A, B). With excess blocking agent (Aca-BN(7-14), 300 µg/mouse), significant reduction of tumor uptake was observed from the images of the blocking group(C), but kidney and bladder (urine) uptake remained high.

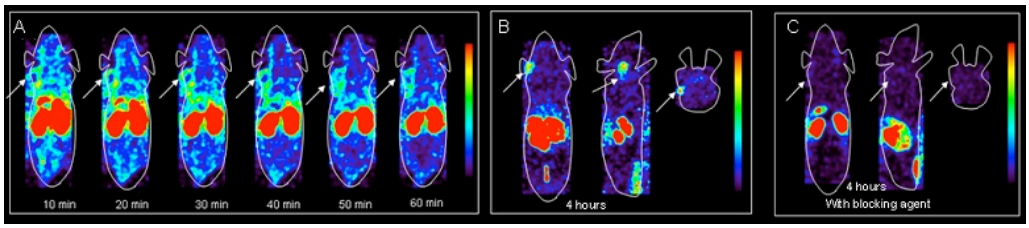

Figure 7: Dynamic coronal microSPECT images of ^{99m}Tc-HABN$_2$ on PC-3 tumor bearing athymic mice during first hour after injection without blocking agent (A) (10 min/frame). Static coronal, sagittal and axial images of ^{99m}Tc-HABN$_2$ on PC-3 tumor bearing mice without (B) and with blocking agent (C) at 4 h after injection. Arrows pointed at the tumor.

DISCUSSION

Dimerization was applied to evaluate a new dimeric bombesin with 2 identical Aca-Bombesin(7–14) units for its GRPR targeting characteristics as a potential imaging agent for prostate cancer. A side by side comparison of the *in vitro* and *in vivo* behavior of monomer and dimer is listed in table 1.

	^{99m}Tc-HABN	**^{99m}Tc-HABN$_2$**
IC_{50} (nM) [a]	12.81±1.34	63.40 ± 11.70
In vitro stability (in human serum)	Stable in 6 h	Stable in 6 h
Log D value	-1.60 ±0.06	-1.54 ± 0.16
Highest cellular uptake (% of incubation dose)	10.9 ± 0.7 [b]	32.5 ± 1.8 [c]
Half-life of efflux (min)	37	84
Tumor uptake (%ID/g)	1.51±0.38	1.58 ± 0.18

Kidney uptake (%ID/g)	6.39±0.83	10.07±1.76
Pancreas uptake (%ID/g)	8.92±1.74	11.26±4.11
Tumor-to-muscle ratio	13.92	3.70

Table 1: ***In vitro*** **and** ***in vivo*** **behavior of bombesin monomer (15) and dimer.**

Uptake values (in %ID/g) and T/NT ratios are determined in several organs and PC-3 tumor at 1h p.i. unless stated otherwise; a= IC_{50} determined with HYNIC conjugations (HYNIC-Aca-BN(7-14) or HYNIC-Glu[Aca-BN(7-14)]$_2$); b=cellular uptake value determined at 1 h post incubation; c= cellular uptake value determined at 4 h post incubation.

In a comparative binding assay, bombesin dimer replaced 50% binding of ^{125}I-tyr^4-BN(1-14) from the GRP receptors in relatively higher nanomolar concentration (31.4 ± 0.4 nM) than the corresponding monomer (Ananias et al. 2011). HYNIC conjugation showed similar slightly negative effect on binding affinity of HYNIC-Glu[Aca-BN(7-14)]$_2$. The additional Aca-BN(7-14) motif and the linker may not be sufficiently flexible to fit in the binding pocket of the GRP receptor as compared to the monomer. The linker may be too short thereby causing steric hindrance upon binding of the molecule to the receptor. However the IC_{50} of HYNIC-Glu[Aca-BN(7-14)]$_2$ is still in an acceptable range. Thus, we decided to label bombesin homodimer with ^{99m}Tc for in vitro and in vivo characterizations. Although development of PET facilities and radiotracers for PET imaging is blooming nowadays, developing new tracers for SPECT imaging is still important because of the availability of SPECT in most areas all over the world. Due to the favorable radioisotope characters and widespread clinical use, we chose to use the γ-emitting isotope ^{99m}Tc. As we reported in previous study (15), the HYNIC/tricine/TPPTS complex was used to serve as chelator for our new tracer because of its high labeling efficiency (rapid and high yield radiolabeling), high solution stability and relatively easy use (12,15,27). It was also chosen because of its hydrophilic character leading to the preferred excretion route via the renal-urinary system. Although urinary activity can limit the clinical use in the pelvic and retroperitoneal areas, this limitation will not be relevant for evaluation of metastases in the skeleton.

^{99m}Tc-HABN$_2$ was prepared with high purity. Due to the same ^{99m}Tc labeling core, monomer and dimer shared similar character in labeling, hydrophilicity and solution stability in saline, cysteine and human serum. However, we noticed that several days of incubation is necessary to complete the conjugation of the HYNIC chelator to the bombesin homodimer due to the position of active glutamic acid. The slightly lower rate of ^{99m}Tc-HYNIC(Tricine/TPPTS)-Glu[Aca-BN(7-14)]$_2$ complex construction may be caused for the same reason. The in vitro cellular uptake, internalization and efflux kinetics were evaluated using the GRPR-expressing human prostate cancer cell line PC-3. Although the binding affinity of bombesin homodimer was 10 times lower than monomer, the specific accumulation of ^{99m}Tc-HABN$_2$ showed almost a linear increase during 4 h experiment period with highest cellular uptake of 32.5 ± 1.8 % added activity (3-fold as high as that of ^{99m}Tc-HABN), whereas that of ^{99m}Tc-HABN reached an uptake plateau in 30 min, which may be due to the higher bombesin "local concentration" of the homodimer in the vicinity of the receptor. In the *in vitro* competitive receptor binding assay, PC-3 cells were incubated with the bombesin ligands for 1 h to allow for the replacement of the GRPR-bound of ^{125}I-tyr^4-BN(1-14). Cellular uptake of ^{99m}Tc-HABN$_2$ gradually increased over time and became higher than ^{99m}Tc-HABN only after 1 h post incubation. This finding indicated that ^{99m}Tc-HABN$_2$ may be more suitable for cancer imaging at later time points (for example 4 h, 24 h p.i.). Therefore, we decided to evaluate the biodistribition and SPECT imaging characters of radiolabeled homodimer in a human prostate cancer xenograft bearing mouse animal model till 24 h post injection. For ^{99m}Tc-HABN and ^{99m}Tc-HABN$_2$, tumors are visualized in the first time frame of microSPECT image at 10 min post injection, it reflected the rapid receptor binding and internalization via GRPR. The slightly higher tumor uptake of ^{99m}Tc-HABN$_2$ (0.78±0.26 %ID/g) compared to ^{99m}Tc-HABN (0.67±0.26 %ID/g) at 4h post injection could be attributed to the combination of higher cellular uptake, slower efflux and molecular size effect. Instead of steady decreases over time, the uptake of ^{99m}Tc-HABN$_2$ remains constant high (11.2±4.9 %ID/g at 24 h post injection) in pancreas which may be because of same reasons. Not only in the GRPR expressing tissues but also in the non-GRPR tissues, the ^{99m}Tc-HABN$_2$ showed a longer retention compared to ^{99m}Tc-HABN. The apparent increase in molecular size resulted in an increased circulation

time and slower clearance of the bombesin dimer. The accumulation in blood for ^{99m}Tc-$HABN_2$ was 4 times higher as that for ^{99m}Tc-HABN at 1h post injection. Although T/NT ratios were constantly increasing due to the slower excretion of ^{99m}Tc-$HABN_2$ in tumor than in non-target tissues (Figure 6), it was well feasible to visualize the tumor with the SPECT images till 4 hours post injection. The contrast of tumor in SPECT images is expected to be better at 24 h post injection, but due to the short half-life of ^{99m}Tc, it was not possible to perform the SPECT scan at 24h post injection. Because of the doubled positive charge from 2 Aca-BN(7-14) motifs, the radioactivity accumulation of ^{99m}Tc-$HABN_2$ in kidney remains at high level within 24 hours, with highest accumulation of 15.1±6.4 %ID/g at 4 h post injection and decreased to 4.7±0.9%ID/g at 24 h. The high radioactivity accumulation in kidney and urine observed from SPECT imaging and/or biodistribution results indicate that the ^{99m}Tc-$HABN_2$ was excreted through renal-urine pathway which is consist with other ^{99m}Tc-HYNIC-peptides. The agonist property of ^{99m}Tc-$HABN_2$ was confirmed by its rapid internalization. Although it's still unclear which between agonist and antagonist is more suitable for the imaging of GRPR-expressing cancer. A few radiolabeled bombesin antagonists, such as Demobesin-1 (Schroeder et al. 2010), already showed their superiority to agonists in tumor accumulation, retention of radioactivity and in vivo pharmacokinetics. ^{99m}Tc-$HABN_2$ exhibited comparable tumor accumulation, but less favorable pharmacokinetics In comparison to those antagonists. Further studies which focus on improving the binding affinity and pharmacokinetics of bombesin homodimer are in progress. Recently, series of radiolabeled Arginine-Glycine-Aspartic acid-bombesin (RGD-BBN) heterodimers for the GRPR targeting were reported (14,28–31). Those heterodimers aim to target two types of receptors simultaneously, to enhance tumor contrast when either or both receptor types are expressed. In the RGD-BBN heterodimer molecular containing one bombesin motif and one RGD motif, the RGD motif is responsible for targeting integrin $\alpha_v\beta_3$-receptors which are upregulated on activated tumor endothelial cells and also highly expressed on some tumor cells such as glioblastoma, breast and prostate tumors, malignant melanomas, and ovarian carcinomas (32). Compared to the bombesin monomer or RGD monomer, the heterodimer shows a synergistic effect for in vivo PC-3 tumor targeting in an animal model

(33). However using heterodimers the target specificity of the SPECT or PET image is lost, but general detection of tumor lesions may be improved. The RGD-BBN heterodimer labeled with radiometals (^{68}Ga and ^{64}Cu) showed higher background than ^{18}F-labeled tracer but slower washout and higher tumor uptake in nude mice bearing breast tumors (14). It's worth to explore the potency of different radioisotopes and chelators on the binding properties and pharmacokinetics of bombesin homodimers. Within ^{99m}Tc-HABN$_2$, two identical bombesin ligands were conjugated with glutamic acid. It would be interesting to investigate the effects of linkers with differences in length, lipophilicity and flexibility, on the *in vitro* and *in vivo* behavior of the tracer.

CONCLUSIONS

We successfully developed a ^{99m}Tc labeled homodimeric bombesin tracer which showed binding with acceptable affinity and specificity to the GRP receptor-positive PC-3 prostate cancer cells *in vitro* and *in vivo*. Moreover we have shown its ability of tumor imaging. Further studies on modification of homodimeric bombesin are required. The current dimer is a useful lead compound for this purpose.

Acknowledgements

This work was made possible by a financial contribution from CTMM, project PCMM, project number 03O-203. We thank Chao Wu for technical assistance on microSPECT images reconstruction and D.F. Samplonius for technical assistance on cell culturing, J. W. A. Sijbesma for assisting animal experiments. All animal experiments were approved by the local animal welfare committee in accordance with the Dutch legislation and carried out in accordance with their guidelines.

References

[1] Ferlay J, Autier P, Boniol M, Heanue M, Colombet M, Boyle P. Estimates of the cancer incidence and mortality in Europe in 2006. Ann. Oncol. 2007 Mar;18(3):581–92.

[2] Jemal A, Siegel R, Ward E, Hao Y, Xu J, Murray T, et al. Cancer statistics, 2008. CA. Cancer J. Clin. 58(2):71–96.

[3] Eisenhauer EA, Therasse P, Bogaerts J, Schwartz LH, Sargent D, Ford R, et al. New response evaluation criteria in solid tumors: revised RECIST guideline (version 1.1). Eur. J. Cancer. 2009 Jan;45(2):228–47.

[4] Aprikian AG, Cordon-Cardo C, Fair WR, Reuter VE. Characterization of neuroendocrine differentiation in human benign prostate and prostatic adenocarcinoma. Cancer. 1993 Jun 15;71(12):3952–65.

[5] Price J, Penman E, Wass JA, Rees LH. Bombesin-like immunoreactivity in human gastrointestinal tract. Regul. Pept. 1984 Sep;9(1-2):1–10.

[6] Spindel ER, Chin WW, Price J, Rees LH, Besser GM, Habener JF. Cloning and characterization of cDNAs encoding human gastrin-releasing peptide. Proc. Natl. Acad. Sci. U. S. A. 1984 Sep;81(18):5699–703.

[7] Track NS, Cutz E. Bombesin-like immunoreactivity in developing human lung. Life Sci. 1982 May 3;30(18):1553–6.

[8] Xiao D, Wang J, Hampton LL, Weber HC. The human gastrin-releasing peptide receptor gene structure, its tissue expression and promoter. Gene. 2001 Feb 7;264(1):95–103.

[9] Erspamer V, Erpamer GF, Inselvini M. Some pharmacological actions of alytesin and bombesin. J. Pharm. Pharmacol. 1970 Nov;22(11):875–6.

[10] McDonald TJ, Jörnvall H, Nilsson G, Vagne M, Ghatei M, Bloom SR, et al. Characterization of a gastrin releasing peptide from porcine non-antral gastric tissue. Biochem. Biophys. Res. Commun. 1979 Sep 12;90(1):227–33.

[11] Zhang X, Cai W, Cao F, Schreibmann E, Wu Y, Wu JC, et al. 18F-labeled bombesin analogs for targeting GRP receptor-expressing prostate cancer. J. Nucl. Med. 2006 Mar;47(3):492–501.

[12] Shi J, Jia B, Liu Z, Yang Z, Yu Z, Chen K, et al. 99mTc-labeled bombesin(7-14)NH2 with favorable properties for SPECT imaging of colon cancer. Bioconjug. Chem. 2008 Jun;19(6):1170–8.

[13] Ait-Mohand S, Fournier P, Dumulon-Perreault V, Kiefer GE, Jurek P, Ferreira CL, et al. Evaluation of 64Cu-labeled bifunctional chelate-bombesin conjugates. Bioconjug. Chem. 2011 Aug 17;22(8):1729–35.

[14] Liu Z, Yan Y, Liu S, Wang F, Chen X. 18F, 64Cu, and 68Ga Labeled RGD-Bombesin Heterodimeric Peptides for PET Imaging of Breast Cancer. Bioconjug. Chem. 2009;20(5):1016–25.

[15] Ananias HJK, Yu Z, Dierckx RA, van der Wiele C, Helfrich W, Wang F, et al. (99m)technetium-HYNIC(tricine/TPPTS)-Aca-bombesin(7-14) as a targeted imaging agent with microSPECT in a PC-3 prostate cancer xenograft model. Mol. Pharm. 2011 Aug 1;8(4):1165–73.

[16] Kramer RH, Karpen JW. Spanning binding sites on allosteric proteins with polymer-linked ligand dimers. Nature. 1998 Oct 15;395(6703):710–3.

[17] Handl HL, Vagner J, Han H, Mash E, Hruby VJ, Gillies RJ. Hitting multiple targets with multimeric ligands. Expert Opin. Ther. Targets. Expert Opinion; 2004;8(6):565–86.

[18] Mulder A, Huskens J, Reinhoudt DN. Multivalency in supramolecular chemistry and nanofabrication. Org. Biomol. Chem. The Royal Society of Chemistry; 2004;2(23):3409–24.

[19] Vance D, Shah M, Joshi A, Kane RS. Polyvalency: a promising strategy for drug design. Biotechnol. Bioeng. 2008 Oct 15;101(3):429–34.

[20] Joosten JAF, Loimaranta V, Appeldoorn CCM, Haataja S, El Maate FA, Liskamp RMJ, et al. Inhibition of Streptococcus suis adhesion by dendritic galabiose compounds at low nanomolar concentration. J. Med. Chem. 2004 Dec 16;47(26):6499–508.

[21] Liu Z, Shi J, Jia B, Yu Z, Liu Y, Zhao H, et al. Two ^{90}Y-labeled multimeric RGD peptides RGD4 and 3PRGD2 for integrin targeted radionuclide therapy. Mol. Pharm. 2011 Apr 4;8(2):591–9.

[22] Chang E, Liu S, Gowrishankar G, Yaghoubi S, Wedgeworth JP, Chin F, et al. Reproducibility study of [(18)F]FPP(RGD)2 uptake in murine models of human tumor xenografts. Eur. J. Nucl. Med. Mol. Imaging. 2011 Apr;38(4):722–30.

[23] Dijkgraaf I, Yim C-B, Franssen GM, Schuit RC, Luurtsema G, Liu S, et al. PET imaging of αvβ3 integrin expression in tumors with 68Ga-labelled mono-, di- and tetrameric RGD peptides. Eur. J. Nucl. Med. Mol. Imaging. 2011 Jan;38(1):128–37.

[24] Shi J, Kim Y-S, Zhai S, Liu Z, Chen X, Liu S. Improving tumor uptake and pharmacokinetics of (64)Cu-labeled cyclic RGD peptide dimers with Gly(3) and PEG(4) linkers. Bioconjug. Chem. 2009 Apr;20(4):750–9.

[25] Dijkgraaf I, Kruijtzer JAW, Liu S, Soede AC, Oyen WJG, Corstens FHM, et al. Improved targeting of the alpha(v)beta (3) integrin by multimerisation of RGD peptides. Eur. J. Nucl. Med. Mol. Imaging. 2007 Feb;34(2):267–73.

[26] Dijkgraaf I, Rijnders AY, Soede A, Dechesne AC, van Esse GW, Brouwer AJ, et al. Synthesis of DOTA-conjugated multivalent cyclic-RGD peptide dendrimers via 1,3-dipolar cycloaddition and their biological evaluation: implications for tumor targeting and tumor imaging purposes. Org. Biomol. Chem. 2007;5(6):935–44.

[27] Liu S, Kim Y-S, Hsieh W-Y, Gupta Sreerama S. Coligand effects on the solution stability, biodistribution and metabolism of the (99m)Tc-labeled cyclic RGDfK tetramer. Nucl. Med. Biol. 2008 Jan;35(1):111–21.

[28] Liu Z, Li Z-B, Cao Q, Liu S, Wang F, Chen X. Small-Animal PET of Tumors with 64Cu-Labeled RGD-Bombesin Heterodimer. J. Nucl. Med. 2009;50(7):1168–77.

[29] Liu Z, Yan Y, Chin FT, Wang F, Chen X. Dual integrin and gastrin-releasing peptide receptor targeted tumor imaging using 18F-labeled PEGylated RGD-bombesin heterodimer 18F-FB-PEG3-Glu-RGD-BBN. J. Med. Chem. 2009 Jan 22;52(2):425–32.

[30] Liu Z, Niu G, Wang F, Chen X. (68)Ga-labeled NOTA-RGD-BBN peptide for dual integrin and GRPR-targeted tumor imaging. Eur. J. Nucl. Med. Mol. Imaging. 2009 Sep;36(9):1483–94.

[31] Li Z-B, Chen K, Chen X. 68Ga-labeled multimeric RGD peptides for microPET imaging of integrin αvβ3 expression. Eur. J. Nucl. Med. Mol. Imaging. Springer Science & Business Media B.V; 2008;35(6):1100–8.

[32] Hynes RO. Integrins: bidirectional, allosteric signaling machines. Cell. 2002 Sep 20;110(6):673–87.

[33] Li Z-B, Wu Z, Chen K, Ryu EK, Chen X. 18F-Labeled BBN-RGD Heterodimer for Prostate Cancer Imaging. J. Nucl. Med. 2008;49(3):453–61.